Published in "Langmuir 32(19): 4896–4903, 2016"
which should be cited to refer to this work.

Vesicle Origami and the Influence of Cholesterol on Lipid Packing

Radu Tanasescu,[†] Martin A. Lanz,[†] Dennis Mueller,[†] Stephanie Tassler,[‡] Takashi Ishikawa,[§] Renate Reiter,[*,∥,⊥] Gerald Brezesinski,[*,‡] and Andreas Zumbuehl[*,†]

[†]Department of Chemistry, University of Fribourg, Chemin du Musée 9, 1700 Fribourg, Switzerland
[‡]Max Planck Institute of Colloids and Interfaces, Science Park Potsdam-Golm, 14476 Potsdam, Germany
[§]Paul Scherrer Institute (PSI), OFLB/010 5232 Villigen PSI, Switzerland
[∥]Experimental Polymer Physics, University of Freiburg, Hermann Herder Strasse 3, 79104 Freiburg, Germany
[⊥]Freiburg Centre for Interactive Materials and Bioinspired Technologies (FIT), 79110 Freiburg, Germany

Supporting Information

ABSTRACT: The artificial phospholipid Pad-PC-Pad was analyzed in 2D (monolayers at the air/water interface) and 3D (aqueous lipid dispersions) systems. In the gel phase, the two leaflets of a Pad-PC-Pad bilayer interdigitate completely, and the hydrophobic bilayer region has a thickness comparable to the length of a single phospholipid acyl chain. This leads to a stiff membrane with no spontaneous curvature. Forced into a vesicular structure, Pad-PC-Pad has faceted geometry, and in its extreme form, tetrahedral vesicles were found as predicted a decade ago. Above the main transition temperature, a noninterdigitated L_α phase with fluid chains has been observed. The addition of cholesterol leads to a slight decrease of the main transition temperature and a gradual decrease in the transition enthalpy until the transition vanishes at 40 mol % cholesterol in the mixture. Additionally, cholesterol pulls the chains apart, and a noninterdigitated gel phase is observed. In monolayers, cholesterol has an ordering effect on liquid-expanded phases and disorders condensed phases. The wavenumbers of the methylene stretching vibration indicate the formation of a liquid-ordered phase in mixtures with 40 mol % cholesterol.

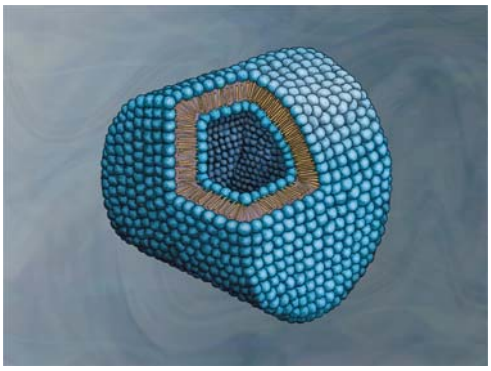

INTRODUCTION

Vesicle origami or the guided self-assembly of a soft matter liposome may lead to materials with unprecedented properties. However, imposing a specific form on a liposome remains a formidable challenge. To achieve this goal, more fundamental insight into the forces determining the local curvature in membranes is needed.

Here, we analyze the effects of membrane interdigitation and the deinterdigitating effect of cholesterol on monolayers and bilayers. Moreover, the liquid-ordered phase is characterized in unprecedented clarity.

Cholesterol is a flat molecule maximizing the hydrophobic forces in model phospholipid membranes.[1] Cholesterol hereby acts as a fluidity buffer,[2] and this leveling effect leads to a liquid-ordered membrane phase.[3] In a nonideal mixture of low- and high-melting glycerophospholipids, cholesterol associates preferentially with the high-melting, saturated lipids.[4] Cholesterol and the glycerophospholipids interact strongly but transiently[5] via (i) hydrogen bonds between the hydroxy group of cholesterol and the phospholipid phosphodiester,[6] (ii) hydrogen bonds among the hydroxy group of cholesterol, water, and the *sn*-1 carbonyl moiety of the phospholipid,[7] (iii) van der Waals hydrophobic forces between the planar cholesterol ring system and the *sn*-1 chain of the phospholipid,[8] and, most importantly, (iv) van der Waals forces between the fatty acyl chains and the cholesterol side chain.[9] The interactions are strongly dependent on the type of phospholipid headgroup and lipid tail saturation[10] and may lead to a positioning of cholesterol in the middle of the bilayer membrane in the presence of polyunsaturated phospholipids.[11]

Here, we discuss the effect of cholesterol on monolayers and bilayers formed by artificial 1,3-diamidophospholipid Pad-PC-Pad (structures in Figure 1). By itself, Pad-PC-Pad forms completely interdigitated bilayer membranes, and the addition of cholesterol should modify this rigid membrane phase, leading to a more fluid liquid-ordered state that we can now show clearly. This raftlike structure would then imply that the bis-amide Pad-PC-Pad shares similarities with the monoamide sphingomyelin or at least that the interaction of Pad-PC-Pad with cholesterol is intermediate with respect to the interaction of sphingomyelin with cholesterol and glycerophospholipids with cholesterol. Overall, the presence of a liquid-ordered membrane phase would imply that cholesterol dominates the

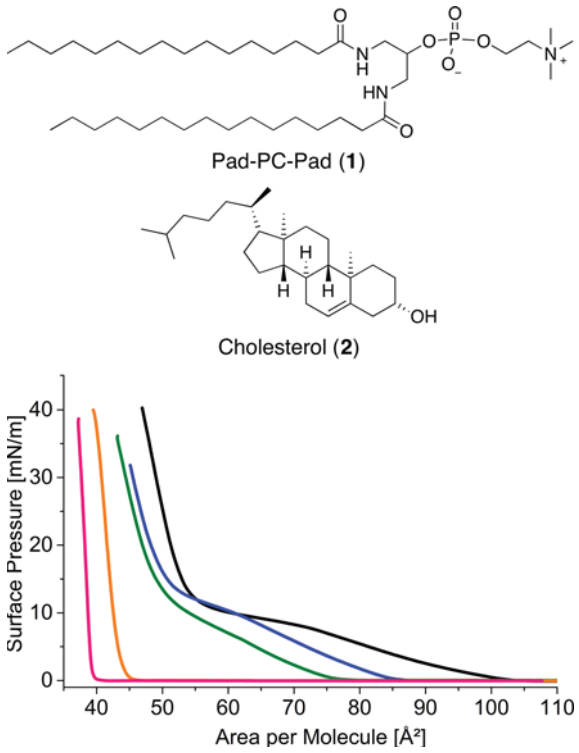

Figure 1. (Top) Chemical structures of 1,3-diamidophospholipid Pad-PC-Pad (1) and cholesterol (2). (Bottom) Surface pressure/molecular area isotherms on water at 10 °C (black, Pad-PC-Pad; blue, Pad-PC-Pad with 10 mol % cholesterol; green, Pad-PC-Pad with 20 mol % cholesterol; orange, Pad-PC-Pad with 40 mol % cholesterol; pink, cholesterol).

interactions with other lipids and that this interaction is not limited to natural lipids.

Pad-PC-Pad can form faceted vesicles.[12,13] We give experimental details on d-form vesicles and a triangular vesicular structure that previously was only alluded to on a much larger scale in a review[14] and has been proposed on the basis of computational studies.[15] Together with icosahedral catanionic vesicles[16] and block copolymer cubes,[17] self-assembly vesicle origami comes of age.

RESULTS AND DISCUSSION

Surface Pressure/Molecular Area Isotherms. Monolayers at the air/water interface of a Langmuir–Pockels trough represent a good starting point for model membrane characterization. The surface pressure/molecular area isotherm for pure Pad-PC-Pad lifts off from a coexisting gas analog (G) and liquid-expanded (LE) phase. (See Figure 1 for 10 °C.) Brewster angle microscopy measurements (Figure S1) confirm this phase coexistence. Pad-PC-Pad exhibits a plateau at approximately 10 mN·m^{-1} on water at 10 °C. This plateau describes a first-order phase transition from an LE to a liquid-condensed (LC) phase and is an additional coexistence region; crystalline domains within a fluid matrix are clearly revealed with Brewster angle microscopy (BAM).[12] The plateau is characterized by a large change in molecular area and almost no change in lateral pressure.

Pure cholesterol remains in coexisting G and LC phases up to an area of 40 Å^2 per molecule. Domains of condensed cholesterol are continuously growing until they cover the entire surface. At a critical area of approximately 38 Å^2/molecule, the surface pressure lifts off into a condensed phase, which is in agreement with previous findings.[18] It has to be noted that monolayer measurements performed under different experimental conditions are difficult to compare, and other researchers report values of about 44 Å^2/molecule for cholesterol.[19,20]

The mixtures of Pad-PC-Pad and cholesterol exhibit intermediate behavior: Pad-PC-Pad with 10 mol % cholesterol lifts off at a smaller area per molecule than pure Pad-PC-Pad, and the phase transition pressure is also slightly higher (11.5 mN·m^{-1}). The plateau is more tilted, pointing to a clearly reduced cooperativity of the transition process. For Pad-PC-Pad with 20 mol % admixed cholesterol, a clear first-order transition is no longer observed. Instead, there is a broad and steeper region in the isotherm that could be an indication of a stepwise transition. The same behavior is observed in mixed DPPC/cholesterol monolayers.[21]

Adding 40 mol % cholesterol, the mixed isotherms look very similar to those of pure cholesterol, indicating that the mixtures have properties clearly dominated by cholesterol. The mixing of the two lipids should be facilitated by the known preference of cholesterol to mix ideally with phosphatidylcholines with a 14–17 carbon chain length.[22] If two lipids mix ideally in a monolayer,[23] then the excess area per molecule A_{ex} is zero and no cholesterol-induced condensation effect is measured.[24]

$$A_{ex} = A_{Pad/Chol} - (x_{Pad}A_{Pad} + x_{Chol}A_{Chol})$$

with $A_{Pad/Chol}$ being the measured mean area of the molecules in a mixed monolayer at a given surface pressure. A_{Pad} and A_{Chol} are the areas of the individual molecules (Pad-PC-Pad and cholesterol, respectively) in single-component monolayers. x_{Pad} and x_{Chol} are the molar fractions of the individual components. The same would be observed if the two components are totally immiscible. Figure 2 shows the excess areas plotted as a

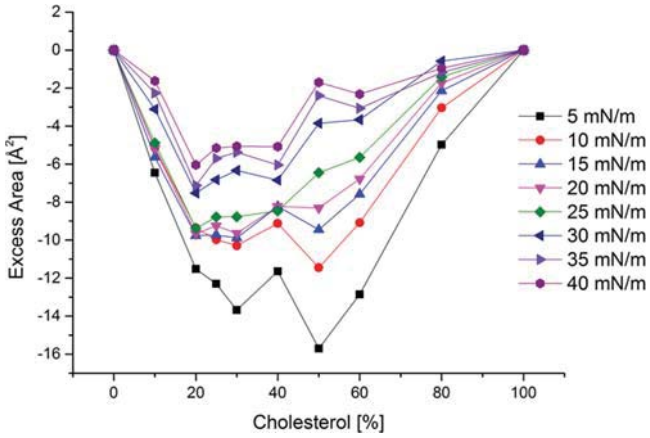

Figure 2. Excess molecular area found at different surface pressures at 20 °C. A value lower than zero shows the condensation effect of cholesterol on Pad-PC-Pad.

function of cholesterol content extracted from molecular area/surface pressure isotherms for isobaric contour lines. It is evident that an area condensation is measured at all surface pressures, indicating preferred interactions between Pad-PC-Pad and cholesterol. The largest condensation can be found at low surface pressures at which the lipid chains seem to be more disorganized and more prone to be organized by the addition of cholesterol (in perfect agreement with the infrared reflection

absorption spectroscopy data that will be discussed below). Figure 2 shows a minimum at a Pad-PC-Pad/cholesterol molar fraction of 2:1. A similar 2:1 complex is also found for DPPC/cholesterol and sphingomyelins/cholesterol and has been related to an umbrella effect of the headgroups shielding one cholesterol from the bulk water phase.[25] Interestingly, the Brewster angle micrograph of the Pad-PC-Pad/cholesterol molar fraction of 2:1 does not display phase separation, even at the lowest surface pressures measured (Figure S1), again indicating that this 2:1 complex represents an optimized interaction between cholesterol and Pad-PC-Pad.

Infrared Reflection Absorption Spectroscopy (IRRAS). An additional monolayer characterization method that was applied was IRRAS: the positions of the symmetric CH_2 stretching vibrational band of Pad-PC-Pad and selected mixtures with cholesterol are plotted against the lateral pressure in Figure 3. At low surface pressures, the wavenumber of the

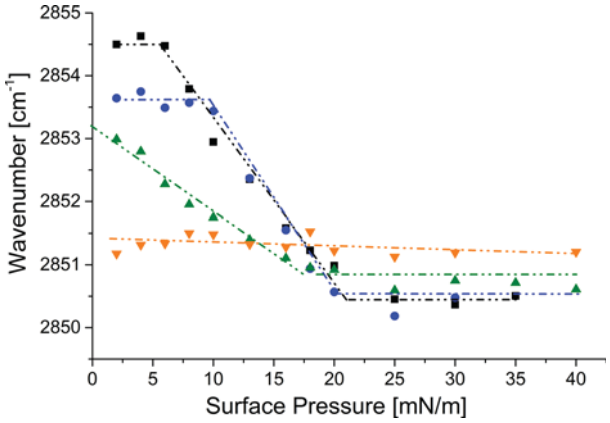

Figure 3. Wavenumbers of the symmetric CH_2 stretching vibrational band (maximum of the Lorentzian function) on water at 10 °C. (black ■) Pad-PC-Pad, (blue ●) Pad-PC-Pad with 10 mol % cholesterol, (green ▲) Pad-PC-Pad with 20 mol % cholesterol, and (orange ▼) Pad-PC-Pad with 40 mol % cholesterol; dotted lines are guides for the eyes. Angle of incidence, 40°; p-polarized IR light.

symmetric CH_2 stretching vibration band of pure Pad-PC-Pad is 2854.5 cm^{-1} and refers to alkyl chains in the gauche conformation (fluid-phase state). With increasing lateral pressure, the wavenumber decreases drastically between 10 and 20 mN/m and remains at 2850.5 cm^{-1} in the condensed state. This low wavenumber indicates that the alkyl chains are in an antiperiplanar (all-trans) conformation. It is worth mentioning that the transition plateau measured by IRRAS seems to be broader than the one determined from the isotherm.

Adding cholesterol immediately starts to order the fluid membrane. At 10 mol % cholesterol, the wavenumber drops by 1 cm^{-1}. The condensed state is almost not affected. At 40 mol % cholesterol, the LE and LC states cannot be distinguished anymore. The wavenumber is almost independent of the pressure and has a value typical for a liquid-ordered phase.

Differential Scanning Calorimetry. To characterize the influence of cholesterol on the lipid packing in Pad-PC-Pad bilayers, we formulated multilamellar vesicles (MLVs) and performed calorimetric experiments using a differential scanning calorimeter (DSC, see Figure 4). Pure Pad-PC-Pad showed an asymmetric phase-transition peak, which can be

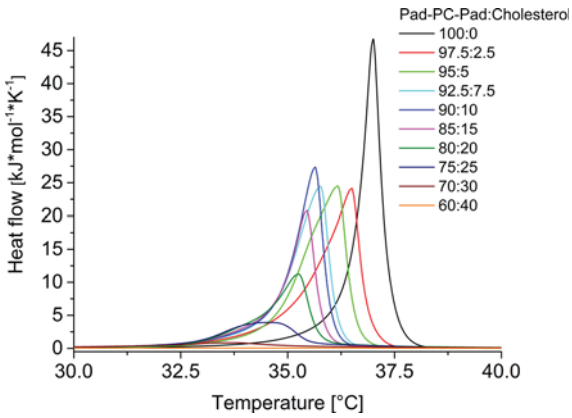

Figure 4. Differential scanning calorimetry scans of mixtures of Pad-PC-Pad and cholesterol. Molecular ratios of the lipids and the corresponding color coding are given.

explained by a gradual dissipation of amide−amide hydrogen bonds resulting from the presence of two hydrogen bond acceptors and two donors in the same molecule.

With a growing percentage of admixed cholesterol, the DSC peaks gradually broadened, hinting at a continuous loss of cooperativity during the main phase transition.[10,26] The main transition temperature decreases linearly with increasing cholesterol concentration, with a slow decrease until 20 mol % cholesterol and a more rapid decrease beyond this value. This phenomenon has already been described for the DPPC natural analog.[27,26] The main phase transition was nearly absent at and above 30 mol % cholesterol. No transition was observed for the mixture with 40 mol % cholesterol.

SAXS and WAXS Bilayer Data. Figure S2 depicts the small-angle X-ray scattering (SAXS) pattern of Pad-PC-Pad at temperatures below (15 °C) and above (40 °C) the main phase-transition temperature (T_m = 37 °C) from the gel to the liquid-crystalline state. For the gel state, a lamellar phase can be detected with Bragg peaks in the ratio of 1:2:3:4. The repeat distance d has been calculated from the q values of the peaks and is presented as a function of temperature in Figure 5 for pure Pad-PC-Pad as well as for selected mixtures with cholesterol. The phase transition of Pad-PC-Pad from the gel to the liquid-crystalline phase state results in a remarkable jump in d by about 25 Å. The liquid-crystalline phase is still lamellar,

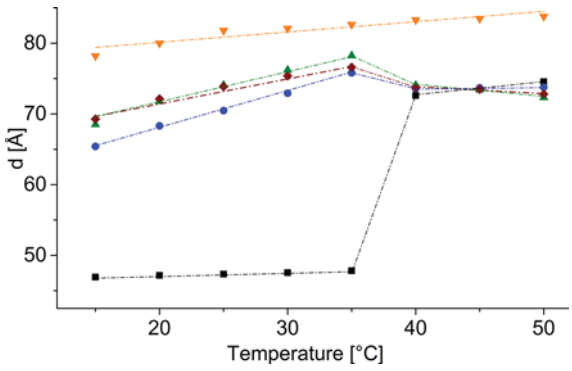

Figure 5. Bilayer spacing d as a function of temperature. (black ■) Pad-PC-Pad, (blue ●) Pad-PC-Pad with 10 mol % cholesterol, (green ▲) Pad-PC-Pad with 20 mol % cholesterol, (red ♦) Pad-PC-Pad with 30 mol % cholesterol, and (orange ▼) Pad-PC-Pad with 40 mol % cholesterol, dotted lines are for guiding the eyes only.

but the broader SAXS peaks indicate a shorter correlation length. Additionally, the increased scattering intensity between the Bragg peaks might indicate the coexistence of correlated and uncorrelated bilayers. The peak positions are listed in Table TS1. The unusually small d value of ~47 Å can be explained by a membrane interdigitation below T_m.[13] The interdigitation is promoted by the 1,3 spacing of the acyl chains in Pad-PC-Pad compared to the tighter 1,2 spacing in natural lipids such as DPPC. This assumption is supported by the results obtained with 1,3-DPPC, which between 30 and 35 °C exhibits an interdigitated gel phase (d = 47 Å) with hexagonal chain packing.[28−30] To prove the interdigitation, the electron density profile (Figure 6) has been derived from the experimental data using the program GAP 1.3, developed by Georg Pabst.[31,32] GAP is capable of analyzing SAXS data of lamellar phases. The model consists of three Gaussians representing the two polar headgroup regions and the alkyl chains between the headgroups in a bilayer. The decomposition of lamellar spacing d into contributions from the bilayer and the interbilayer water is not trivial because the electron density profiles, reconstructed from the diffraction patterns, are of low resolution. Here, the bilayer spacing is determined to be $d_B = 2(z_H + \sigma_H)$ as illustrated in Figure 6. With z_H = 13.5 Å and σ_H = 3.5 Å, the bilayer of 34 Å is extremely thin. Translating $2\sigma_H$ directly into the headgroup thickness of 7 Å, the hydrophobic region is only 20 Å thick. For chains in the all-antiperiplanar (all-trans) conformation, the assumed length is 1.265 Å per CH_2 and 1.54 Å for the terminal CH_3 group.[33] This leads to a chain length of approximately 19.3 Å (without the amide-C function). Therefore, a complete bilayer membrane interdigitation has to be assumed for Pad-PC-Pad. The thickness increase of 25 Å upon membrane melting is fully consistent with noninterdigitated C_{16} chains in a fluid state and an additional incorporation of water between the bilayers. In comparison, d values of 63.7 Å ($L_{\beta'}$ at 20 °C) and 65.8 Å (L_α at 50 °C) have been determined for aqueous 1,2-DPPC dispersions.[34] In contrast, 1,3-DPPC exhibits much smaller d values in the interdigitated gel phase but very similar d values in the L_α phase (65 Å). The almost 10-Å-thicker bilayer of Pad-PC-Pad in the L_α phase indicates the incorporation of a much larger water layer between the lipid bilayers compared to that between the glycerophospholipids.

The incorporation of cholesterol has a strong impact on the bilayer spacing, and with increasing amounts of cholesterol, the d value increases (Figure 5). Obviously, the interdigitation of chains is disturbed by the presence of cholesterol. The bilayer spacing increases slightly with increasing temperature. The main transition is accompanied by only a marginal decrease in d, which has the same values in the liquid-crystalline state as pure Pad-PC-Pad bilayers. In the case of 40 mol % cholesterol, no transition is observable, in perfect agreement with the DSC curves. Only a slight and continuous increase in the bilayer spacing can be seen. The reason is the additional incorporation of water due to increased mobility at higher temperature.

The wide-angle X-ray scattering (WAXS) patterns of Pad-PC-Pad and the mixtures with cholesterol are shown in Figures S3 and S4 temperatures below (15 °C) and above (40 °C) the main phase-transition temperature. One Bragg peak at ~1.5 $Å^{-1}$ is detectable at 15 °C (gel state), and at 40 °C, only a broad halo can be found at 1.38 $Å^{-1}$ for pure Pad-PC-Pad. The peak positions in the WAXS pattern are listed in Table TS2. The single peak in the gel state indicates the hexagonal packing of nontilted chains. This is consistent with fully interdigitated chains in the gel state. The corresponding cross-sectional area

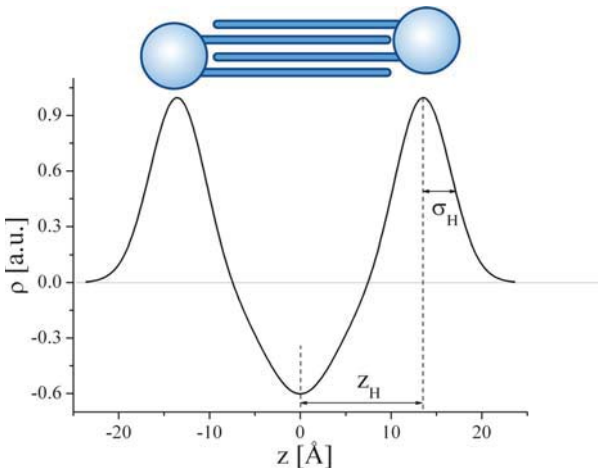

Figure 6. Electron density profile of the Pad-PC-Pad bilayer depicting the complete interdigitation below the main transition temperature.

per chain of 20.1 $Å^2$ is the same as observed for 1,3-DPPC. The molten chains, characterized by the broad halo, exhibit an averaged cross-sectional area of 23.9 $Å^2$.

For mixtures with cholesterol, the intensity of the Bragg peaks in WAXS decreases with increasing cholesterol content, and with 40 mol % cholesterol, no peaks can be determined. In the case of 10 and 20 mol % cholesterol, three Bragg peaks have been observed, which can be explained by an oblique unit cell of the chains in the gel state instead of the hexagonal packing observed for pure Pad-PC-Pad. The cross-sectional area of the hydrophobic lipid chains in the cholesterol-containing samples increases gradually with increasing cholesterol content to 20.7 $Å^2$ (20 mol % cholesterol), in perfect agreement with the results obtained in the 2D monolayers.

Cryo-Transmission Electron Micrographs. The cryo-transmission electron micrographs show a clear effect of cholesterol on the Pad-PC-Pad vesicle geometry (Figure 7). The vesicles formulated from pure Pad-PC-Pad show faceted geometry (Figure 7D). This is due to membrane leaflet

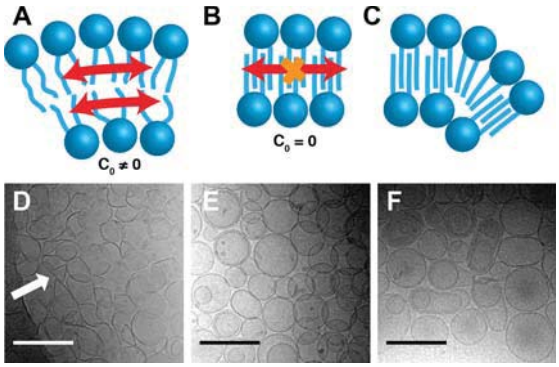

Figure 7. (A) Typical spherical vesicles are formed if the bilayer membrane leaflets are independent of each other and overall positive curvature C_0 is found. (B) Pad-PC-Pad membranes show no spontaneous curvature and are completely interdigitated. (C) A closed Pad-PC-Pad vesicle forms only if the inner membrane leaflet is broken. Cryo electron micrographs of extruded vesicles from pure Pad-PC-Pad (D), Pad-PC-Pad and 10 mol % cholesterol (E), and Pad-PC-Pad and 40 mol % cholesterol (F). The change from rigid, faceted vesicles (D) toward highly flexible vesicles (F) is clearly visible. The scale bars are 200 nm. The white arrow points to a triangular vesicle.

interdigitation that leads to rigid, flat membrane faces.[12,13] Standard phospholipid bilayers consist of two independent bilayer leaflets that slide on top of each other. This flexibility is needed for the formation of spherical vesicles. Furthermore, geometry demands a higher number of molecules in the outer membrane leaflet compared to the inner leaflet, leading to positive membrane curvature C_0 (Figure 7A). If, however, the membrane leaflets are interdigitated, then the membrane leaflets are not independent anymore and the spontaneous curvature is zero (Figure 7B). Such a membrane can be forced to form closed vesicles only if the inner leaflet is broken (Figure 7C). The cryo-TEM confirms the theory proposed by Noguchi.[15]

The addition of 10 mol % cholesterol removes membrane interdigitation, and the two bilayer membrane leaflets are again independent of each other, leading to commonly observed round vesicles (Figure 7E). Further addition of cholesterol leads to highly flexible membranes that may even survive the shear forces of an extrusion through 100 nm track-edged filters (Figure 7F).

Cryo-TEM tomography pictures were recorded from a sample of frozen Pad-PC-Pad vesicles by tilting the stage. Figure 8 shows the geometry of the vesicles from the top and the side (Figure 8A,B). The artist's rendering of the vesicle (Figure 8C) depicts a vesicle with nonspherical, nonplatonic geometry with maximized flat facets and sharp edges.

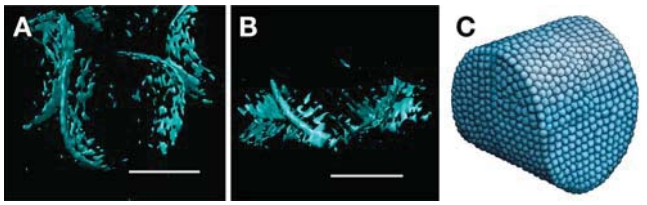

Figure 8. (A) Top and (B) side views of a faceted Pad-PC-Pad vesicle. The artist's rendering in C depicts the special form (d form) of the vesicle that may develop. The scale bars are 50 nm.

Mechanosensitivity of the Vesicle Formulations. Standard Pad-PC-Pad vesicles are mechanosensitive and release an entrapped fluorescent marker upon vortex shaking.[12] The softening of the membranes caused by the addition of 10 mol % cholesterol leads to a leakier membrane both under mechanical stress and at rest (Figure 9). Pad-PC-Pad vesicles containing 10 mol % cholesterol release significantly more of the entrapped dye compared to all other vesicle formulations. At higher cholesterol concentrations, the vesicle membranes retighten and are able to compensate for the lack of membrane interdigitation. The special effect of low cholesterol concentrations on membranes has been noted before in DPPC membranes.[35,36]

CONCLUSIONS

The interactions of artificial 1,3-diamidophospholipid Pad-PC-Pad with cholesterol were probed using various monolayer and bilayer techniques. Overall, the Pad-PC-Pad/cholesterol interactions can be placed in between sphingomyelin/cholesterol and DPPC/cholesterol interactions, and this could make Pad-PC-Pad an interesting tool for chemical biology. Cholesterol has a profound influence on the non-natural Pad-PC-Pad membrane removing the membrane interdigitation and inducing a liquid-ordered phase.

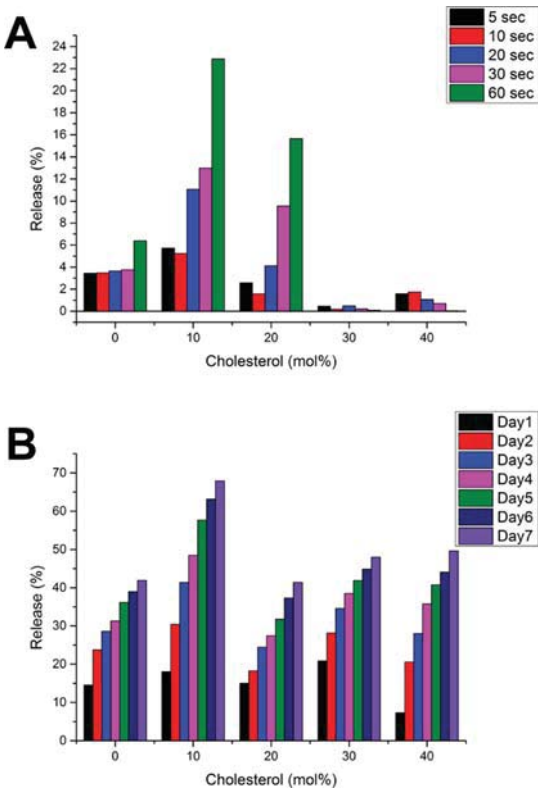

Figure 9. (A) Vortex shaking of vesicle suspensions of Pad-PC-Pad/cholesterol with entrapped 5(6)-carboxyfluorescein leading to dye release. (B) Spontaneous release of vesicle-entrapped 5(6)-carboxyfluorescein over a prolonged time.

EXPERIMENTAL SECTION

Synthesis. The C16 1,3-diamidophospholipid Pad-PC-Pad was synthesized as previously reported.[37] Cholesterol (Sigma grade, ≥99% purity) and chloroform (Chromasolv Plus, HPLC grade, ≥99% purity) were purchased from Sigma-Aldrich.

Surface Pressure/Molecular Area Isotherms. Pressure/area isotherms of monolayers were measured at the air/water interface of a Riegler & Kierstein (Potsdam, Germany) Langmuir–Pockels trough equipped with two moving barriers and a surface pressure microbalance using filter paper or a glass plate as the Wilhelmy plate. Ultrapure water with a specific resistance of 18.2 MΩ·cm was used as a subphase, and the temperature was controlled to a precision of ±0.1 °C as measured in the subphase itself.

Pad-PC-Pad and cholesterol were mixed in chloroform to molar percentages of 0 to 100% cholesterol, and the solvent was removed by low-pressure evaporation. To ensure the removal of residual water and prevent cholesterol oxidation, lipids were dried under vacuum overnight and stored at −20 °C under argon. The phospholipid–cholesterol mixtures were redissolved in chloroform to a final concentration of 550 μM. Fifty microliters were spread on the pre-equilibrated subphase, and the monolayer was incubated for approximately 20 min at a constant area of approximately 100 Å^2/molecule to ensure uniform lipid distribution and solvent evaporation. The monolayer was then compressed at (1.80 ± 0.12) Å^2/(molecule·min) to a final surface pressure. All experiments were performed at least two times from fresh solutions.

Release Experiments. Two milligrams of Pad-PC-Pad were weighed into a 25 mL round-bottomed flask and dissolved in 1 mL of $CHCl_3$. The amount of cholesterol required was added at this point. The solvent was removed under reduced pressure, and the thin film was dried under high vacuum overnight. One milliliter of 5(6)-carboxyfluorescein-containing buffer (10 mM HEPES buffer, 50 mM 5(6)-carboxyfluorescein dissolved in ultrapure water, pH 7.4 (NaOH), 200 mOsm (NaCl/L)) was added, and the film was hydrated for 30

min. Afterward, five freeze/thaw cycles were preformed using liquid nitrogen and a 65 °C water bath. The suspension was extruded 11 times using a miniextruder (Avanti Polar Lipids) and a track-etched filter membrane (100 nm, Whatman). Size exclusion chromatography (PD-10 desalting columns, GE Healthcare) was used to exchange the outer buffer (using 10 mM HEPES dissolved in ultrapure water, pH 7.4 (NaOH), 200 mOsm (NaCl/L)). The purified suspension was diluted to 100 mL with additional outer buffer. Six 2 mL aliquots were used to fill 5 mL vials with PE caps and vortex mixed for different periods of time (0, 5, 10, 20, 30, 60 s) at 2500 rpm. The release of the 5(6)-carboxyfluorescein was quantified using a fluorimeter (HIDEY Sense Microplate Reader) at 485 nm (excitation) and 535 nm (emission). As a control for maximum dye release (F_{100}), 2 vol % of a 10 vol % Triton-X100 solution in ultrapure water was added to an additional sample. The release at time x was calculated with the formula $[F_x - F_0]/[F_{100} - F_0]$, with F_0 being the value at time 0.

Differential Scanning Calorimetry. Differential scanning calorimetry experiments of cholesterol-enriched Pad-PC-Pad multilamellar liposomes were performed using a Nano DSC (TA Instruments). The phospholipid concentration was kept constant (1 mg/mL). Pad-PC-Pad and cholesterol were mixed to molar percentages of 0 to 30% cholesterol in 25 mL round-bottomed flasks, and the solvent was removed by low-pressure evaporation. To ensure the removal of residual water and prevent cholesterol oxidation, the lipid films were dried under vacuum overnight. The liposomes were formulated in >18.2 MΩ·cm Milli-Q water following a previously described method.[15] No extrusion steps were used in order to avoid lipid/cholesterol ratio changes through the loss of material on filters. The lipid concentration in the DSC suspensions was determined using a microwave-based phosphate assay.[16] Samples were degassed for at least 30 min prior to DSC scans using a TA degassing station. Scans were run at 0.5 °C/min from 5 to 60 °C. All experiments were performed at least two times from scratch in order to ensure reproducibility. Four heating/cooling runs were made for each experiment, and the data from the second heating run were taken as the results.

Brewster Angle Microscopy. Brewster angle micrographs were recorded with a commercially available Multiskop (Optrel, Germany) equipped with a Langmuir trough from R & K constructed identically to the one described above. Great care was taken that the investigated films were prepared under the same experimental conditions as for the monolayers that have already been discussed in this article.

Parallel polarized laser light with respect to the plane of incidence of a wavelength of λ = 632.8 nm is reflected on the water surface under the Brewster angle of water (53.1°). The polarizer and analyzer were set to 0° to suppress reflected light from a pure water surface. The reflected beam, which maps the inhomogeneities of the Langmuir film, is focused on a CCD camera for visualization. An objective of 10-fold magnification (Mitutoyo) is mounted on a piezo translation stage that moves continuously to bring consecutive stripes of the image into focus. A streaming video sequence is recorded to construct an overall sharp image. The lipid films were imaged at different stages of monolayer compression.

FT-Infrared Reflection–Absorption Spectroscopy. Infrared reflection–absorption spectra (IRRA spectra) were recorded on a Vertex 70 FT-IR spectrometer (Bruker, Ettlingen, Germany). The setup includes a film balance (R&K, Potsdam, Germany) located inside an enclosed container (external air/water reflection unit XA-511, Bruker). A sample trough with two movable barriers and a reference trough (subphase without a monolayer) allow the fast recording of sample and reference spectra by a shuttle technique. The infrared beam is focused on the liquid surface by a set of mirrors. The angle of incidence normal to the surface can be varied by moveable arms in the range of 30–72°. A KRS-5 wire grid polarizer is used to polarize the infrared radiation in either the parallel (p) or perpendicular (s) direction. After reflection from the surface, the beam is directed onto a narrow-band mercury–cadmium–telluride (MCT) detector cooled with liquid nitrogen. Reflectance–absorbance spectra were obtained by using $-\log(R/R_0)$, with R being the reflectance of the film-covered surface and R_0 being the reflectance of the same subphase without the film. For each single-beam spectrum, 200 scans (s-polarized light) or 400 scans (p-polarized light) were added with a scanning velocity of 20 kHz and a resolution of 8 cm^{-1}, apodized using the Blackman-Harris 3-term function, and fast Fourier transformed after one level of zero filling. For data analysis, spectra obtained with s-polarized light with a 40° angle of incidence were used. All spectra were corrected for atmospheric interference using the OPUS software and baseline corrected using the spectra-subtraction software. The spectra are not smoothed. The position of the symmetric CH_2 stretching vibration was determined with a Lorentzian function in Origin.

Small-Angle and Wide-Angle X-ray Scattering. The SAXS and WAXS measurements were performed at high-brilliance beamline ID02 at the European Synchrotron Radiation Facility (Grenoble, France). The energy of the incident beam was 12.5 keV (λ= 0.992 Å), the beam size was about 100 μm, and the sample-to detector distance was 1.2 m. The small -angle diffraction patterns were collected by a 4 FT-CCD detector (Rayonix MX-170HS). For SAXS, a q range from 0.006 to 0.65 $Å^{-1}$ with a resolution of 3×10^{-4} $Å^{-1}$ (full-width at half-maximum) was used. WAXS data were carried out from 0.72 to 5.1 $Å^{-1}$. To avoid radiation damage, each sample was measured with 10 frames with an exposure time of 0.05 s per frame. For data analysis, the average of all 10 frames was used. The collected 2D powder diffraction spectra were treated with BH plots (Macro in MathLab) and Origin. These data were then corrected for the empty sample holder and bulk solution. The angular calibration of the SAXS detector was performed with silver behenate powder, and for the WAXS detector (Rayonix LX-170HS), PBBA was used. The temperature was adjusted with a Huber Unistat thermostatic bath (precision of 0.1 °C). Experiments have been performed at 15 to 50 °C in 5 °C steps. The samples were sealed in glass capillaries and well positioned in a Peltier-controlled automatic sample changer.

Pad-PC-Pad and cholesterol were each dissolved in chloroform as 1 mM solutions. These solutions were mixed to give the desired molar ratios. The mixtures were dried under nitrogen flow and vacuum desiccated overnight. The following day, water was added to a final concentration of 20 wt % lipid–cholesterol in 80 wt % water. The dispersions were heated to 50 °C (above T_m = 37 °C) and shaken to ensure proper mixing. Then, the samples were sealed in 1.5 mm glass capillaries with a wall thickness of 1/100 mm (Mark Röhrchen für röntgenographische Aufnahmen, Müller, Berlin, Germany) and stored for 1 week in a refrigerator (4 °C) and 1 week at room temperature.

Cryo-Transmission Electron Microscopy. Cryo-TEM was carried out for $LUVET_{100}$ using a JEM2200FS TEM (JEOL, Japan) at the Electron Microscopy Facility, PSI. The suspension was mounted on glow-discharged holey carbon grids, quickly frozen by a Cryoplunge 3 system (Gatan, USA), and transferred to a JEM2200FS transmission electron microscope (JEOL, Japan) using a Gatan 626 cryo-holder. Cryo-electron micrographs were recorded at an acceleration voltage of 200 kV, at 20 000× magnification with 4–8 μm underfocus and a dose of 10 electrons/$Å^2$ using an F416 CMOS detector (TVIPS, Germany). Tomographic data sets were acquired from −65 to 65° with a 30 electrons/$Å^2$ dose using SerialEM software[38] and reconstructed using IMOD software.[39] The reconstituted structure was presented as a surface-rendered model using UCSF Chimera.[40]

■ ASSOCIATED CONTENT

● Supporting Information

The Supporting Information is available

Brewster angle micrographs and SAXS and WAXS bilayer data (PDF)

■ AUTHOR INFORMATION

Corresponding Authors

*E-mail: renate.reiter@physik.uni-freiburg.de.

*E-mail: brezesinski@mpikg.mpg.de.

*E-mail: andreas.zumbuehl@unifr.ch.

Author Contributions

The manuscript was written through the contributions of all authors.

Funding

The project was funded by a grant from the Swiss National Science Foundation (PP00P2_138926/1) to A.Z.

Notes

The authors declare no competing financial interest.

■ ACKNOWLEDGMENTS

We are thankful for the beam time at High Brilliance Beamline ID02 at the ESRF in Grenoble, France. In particular, we thank Dr. Gudrun Lotze for her ambitious support at the beamline. We thank Irina Berndt (MPI-KG) for precise monolayer measurements at the air−water interface. A.Z. acknowledges participation in the National Centers for Competence in Research Chemical Biology and Bio-Inspired Materials funded by the Swiss National Science Foundation.

■ REFERENCES

(1) Krause, M. R.; Turkyilmaz, S.; Regen, S. L. Surface Occupancy Plays a Major Role in Cholesterol's Condensing Effect. *Langmuir* **2013**, *29*, 10303−10306.

(2) Chen, C.; Han, D.; Cai, C.; Tang, X. An Overview of Liposome Lyophilization and its Future Potential. *J. Controlled Release* **2010**, *142*, 299−311.

(3) Mouritsen, O. G. The Liquid-Ordered State Comes of Age. *Biochim. Biophys. Acta, Biomembr.* **2010**, *1798*, 1286−1288.

(4) Krause, M. R.; Daly, T. A.; Almeida, P. F.; Regen, S. L. Push-Pull mechanism for Lipid Raft Formation. *Langmuir* **2014**, *30*, 3285−3289.

(5) Scheidt, H. A.; Huster, D.; Gawrisch, K. Diffusion of Cholesterol and its Precursors in Lipid Membranes Studied by 1H Pulsed Field Gradient Magic Angle Spinning NMR. *Biophys. J.* **2005**, *89*, 2504−2512.

(6) Soubias, O.; Jolibois, F.; Reat, V.; Milon, A. Understanding Sterol-Membrane Interactions, Part II: Complete 1H and 13C Assignments by Solid-State NMR Spectroscopy and Determination of the Hydrogen-Bonding Partners of Cholesterol in a Lipid Bilayer. *Chem. - Eur. J.* **2004**, *10*, 6005−6014.

(7) Pasenkiewicz-Gierula, M.; Rog, T.; Kitamura, K.; Kusumi, A. Cholesterol Effects on the Phosphatidylcholine Bilayer Polar Region: A Molecular Simulation Study. *Biophys. J.* **2000**, *78*, 1376−1389.

(8) Huster, D.; Arnold, K.; Gawrisch, K. Influence of Docosahexaenoic Acid and Cholesterol on Lateral Lipid Organization in Phospholipid Mixtures. *Biochemistry* **1998**, *37*, 17299−17308.

(9) Scheidt, H. A.; Meyer, T.; Nikolaus, J.; Baek, D. J.; Haralampiev, I.; Thomas, L.; Bittman, R.; Muller, P.; Herrmann, A.; Huster, D. Cholesterol's Aliphatic Side Chain Modulates Membrane Properties. *Angew. Chem., Int. Ed.* **2013**, *52*, 12848−12851.

(10) McMullen, T. P. W.; McElhaney, R. N. Differential Scanning Calorimetric Studies of the Interaction of Cholesterol with Distearoyl and Dielaidoyl Molecular Species of Phosphatidylcholine, Phosphatidylethanolamine, and Phosphatidylserine. *Biochemistry* **1997**, *36*, 4979−4986.

(11) Kucerka, N.; Marquardt, D.; Harroun, T. A.; Nieh, M. P.; Wassall, S. R.; Katsaras, J. The Functional Significance of Lipid Diversity: Orientation of Cholesterol in Bilayers is Determined by Lipid Species. *J. Am. Chem. Soc.* **2009**, *131*, 16358−16359.

(12) Holme, M. N.; Fedotenko, I. A.; Abegg, D.; Althaus, J.; Babel, L.; Favarger, F.; Reiter, R.; Tanasescu, R.; Zaffalon, P.-L.; Ziegler, A.; Müller, B.; Saxer, T.; Zumbuehl, A. Shear-Stress Sensitive Lenticular Vesicles for Targeted Drug Delivery. *Nat. Nanotechnol.* **2012**, *7*, 536−543.

(13) Weinberger, A.; Tanasescu, R.; Stefaniu, C.; Fedotenko, I. A.; Favarger, F.; Ishikawa, T.; Brezesinski, G.; Marques, C. M.; Zumbuehl, A. Bilayer Properties of 1,3-Diamidophospholipids. *Langmuir* **2015**, *31*, 1879−1884.

(14) Sackmann, E. Membrane Bending Energy Concept of Vesicle- and Cell-Shapes and Shape-Transitions. *FEBS Lett.* **1994**, *346*, 3−16.

(15) Noguchi, H. Polyhedral Vesicles: a Brownian Dynamics Simulation. *Phys. Rev. E: Stat. Phys., Plasmas, Fluids, Relat. Interdiscip. Top.* **2003**, *67*, 041901.

(16) Dubois, M.; Demé, B.; Gulik-Krzywicki, T.; Dedieu, J. C.; Vautrin, C.; Désert, S.; Perez, E.; Zemb, T. Self-Assembly of Regular Hollow Icosahedra in Salt-Free Catanionic Solutions. *Nature* **2001**, *411*, 672−675.

(17) La, Y.; Park, C.; Shin, T. J.; Joo, S. H.; Kang, S.; Kim, K. T. Colloidal Inverse Bicontinuous Cubic Membranes of Block Copolymers with Tunable Surface Functional Groups. *Nat. Chem.* **2014**, *6*, 534−541.

(18) Shah, D. O.; Schulman, J. H. Influence of Calcium Cholesterol and Unsaturation on Lecithin Monolayers. *J. Lipid Res.* **1967**, *8*, 215−226.

(19) Cadena-Nava, R. D.; Martin-Mirones, J. M.; Vazquez-Martinez, E. A.; Roca, J. A.; Ruiz-Garcia, J. Direct Observations of Phase Changes in Langmuir Films of Cholesterol. *Rev. Mex. Fis.* **2006**, *52*, 32−40.

(20) Kim, K.; Kim, C.; Byun, Y. Preparation of a Dipalmitoylphosphatidylcholine/Cholesterol Langmuir-Blodgett Monolayer that Suppresses Protein Adsorption. *Langmuir* **2001**, *17*, 5066−5070.

(21) Albrecht, O.; Gruler, H.; Sackmann, E. Pressure-Composition Phase Diagrams of Cholesterol/Lecithin, Cholesterol/Phosphatidic Acid, and Lecithin/Phosphatidic Acid mixed Monolayers: a Langmuir Film Balance Study. *J. Colloid Interface Sci.* **1981**, *79*, 319−338.

(22) Mattjus, P.; Hedstrom, G.; Slotte, J. P. Monolayer Interaction of Cholesterol with Phosphatidylcholines - Effects of Phospholipid Acyl-Chain Length. *Chem. Phys. Lipids* **1994**, *74*, 195−203.

(23) Gaines, G. L. Thermodynamic Relationships for Mixed Insoluble Monolayers. *J. Colloid Interface Sci.* **1966**, *21*, 315−319.

(24) Chou, T.-H.; Chang, C.-H. Thermodynamic Behavior and Relaxation Processes of Mixed DPPC/Cholesterol Monolayers at the Air/Water Interface. *Colloids Surf., B* **2000**, *17*, 71−79.

(25) Flasinski, M.; Broniatowski, M.; Majewski, J.; Dynarowicz-Latka, P. X-ray Grazing Incidence Diffraction and Langmuir Monolayer Studies of the Interaction of β-Cyclodextrin with Model Lipid Membranes. *J. Colloid Interface Sci.* **2010**, *348*, 511−521.

(26) Huang, T.-H.; Lee, C. W. B.; Das Gupta, S. K.; Blume, A.; Griffin, R. G. A ^{13}C and ^{2}H Nuclear Magnetic Resonance Study of Phosphatidylcholine/Cholesterol Interactions: Characterization of Liquid-Gel Phases. *Biochemistry* **1993**, *32*, 13277−13287.

(27) Redondo-Morata, L.; Giannotti, M. I.; Sanz, F. Influence of Cholesterol on the Phase Transition of Lipid Bilayers: A Temperature-Controlled Force Spectroscopy Study. *Langmuir* **2012**, *28*, 12851−12860.

(28) Serrallach, E. N.; Dijkman, R.; de Haas, G. H.; Shipley, G. G. Structure and Thermotropic Properties of 1,3-Dipalmitoyl-glycero-2-phosphocholine. *J. Mol. Biol.* **1983**, *170*, 155−174.

(29) Stümpel, J.; Eibl, H.; Nicksch, A. X-Ray Anaylsis And Calorimetry on Phosphatidylcholine Model Membranes The Influence of Length and Position of Acyl Chains upon Structure and Phase Behaviour. *Biochim. Biophys. Acta, Biomembr.* **1983**, *727*, 246−254.

(30) Zumbuehl, A.; Dobner, B.; Brezesinski, G. Phase Behavior of Selected Artificial Lipids. *Curr. Opin. Colloid Interface Sci.* **2014**, *19*, 17−24.

(31) Pabst, G.; Rappolt, M.; Amenitsch, H.; Laggner, P. Structural Information from Multilamellar Liposomes at Full Hydration: Full q-Range Fitting with High Quality x-Ray Data. *Phys. Rev. E: Stat. Phys., Plasmas, Fluids, Relat. Interdiscip. Top.* **2000**, *62*, 4000−4009.

(32) Pabst, G.; Katsaras, J. Structure and Interactions in the Anomalous Swelling Regime of Phospholipid Bilayers. *Langmuir* **2003**, *19*, 1716−1722.

(33) Israelachvili, J. N. *Intermolecular and Surface Forces*, 3rd ed.; Academic Press: San Diego, 2011.

(34) Lucio, M.; Bringezu, F.; Reis, S.; Lima, J. L. F. C.; Brezesinski, G. Binding of Nonsteroidal Anti-Inflammatory Drugs to DPPC: Structure and Thermodynamic Aspects. *Langmuir* **2008**, *24*, 4132−4139.
(35) Mouritsen, O. G.; Zuckermann, M. J. What is so Special about Cholesterol? *Lipids* **2004**, *39*, 1101−1113.
(36) Kim, K.; Choi, S. Q.; Zell, Z. A.; Squires, T. M.; Zasadzinski, J. A. Effect of Cholesterol Nanodomains on Monolayer Morphology and Dynamics. *Proc. Natl. Acad. Sci. U. S. A.* **2013**, *110*, E3054−E3060.
(37) Fedotenko, L. A.; Stefaniu, C.; Brezesinski, G.; Zumbuehl, A. Monolayer Properties of 1,3-Diamidophospholipids. *Langmuir* **2013**, *29*, 9428−9435.
(38) Mastronarde. Automated Electron Microscope Tomography Using Robust Prediction of Specimen Movements. *J. Struct. Biol.* **2005**, *152*, 36−51.
(39) Kremer, J. R.; Mastronarde, D. N.; McIntosh, J. R. Computer Visualization of Three-Dimensional Image Data using IMOD. *J. Struct. Biol.* **1996**, *116*, 71−76.
(40) Pettersen, E. F.; Goddard, T. D.; Huang, C. C.; Couch, G. S.; Greenblatt, D. M.; Meng, E. C.; Ferrin, T. E. UCSF Chimera - A Visualization System for Exploratory Research and Analysis. *J. Comput. Chem.* **2004**, *25*, 1605−1612.